UNIVERSITY OF CALIFORNIA

Santa Barbara

An Engineered Platform to Investigate the Role of the Cell Adhesive Interface on hiPSC-CM Maturity

A Thesis submitted in partial satisfaction of the

requirements for the degree Master of Science

in Mechanical Engineering

by

Kerry Lane

Committee in charge:

Professor Beth Pruitt, Chair

Professor Adele Doyle

Professor Emilie Dressaire

June 2020

The thesis of Kerry Lane is approved.

_____

Emilie Dressaire

_____

Adele Doyle

_____

Beth Pruitt, Committee Chair

April 2020

An Engineered Platform to Investigate the Role of the Cell Adhesive Interface on hiPSC-CM Maturity

ACKNOWLEDGEMENTS

I want to thank my advisor, Beth Pruitt, for supporting me and providing me with encouragement and guidance. I would also like to thank my lab mates for their helpful conversations, advice, and support. Specifically, I want to thank Erica Castillo for being a patient mentor to me and providing me with indispensable advice, discussions, and training. I would also like to thank my committee members, Adele Doyle and Emilie Dressaire, for their advice and discussions on my work.

This material is based upon work supported by the National Science Foundation Graduate Research Fellowship Program under Grant No. 1650114.

ABSTRACT

An Engineered Platform to Investigate the Role of the Cell Adhesive Interface on hiPSC-CM Maturity

by

Kerry Lane

Cell-cell interactions between cardiomyocytes (CMs) are crucial to the structure and function of heart tissue. Due to the force-producing nature of the heart, cell-cell interactions between individual CMs are key to maintaining tissue integrity and mechanotransduction throughout the heart. However, very few studies have focused on CM-CM mechanobiology, and those studies have used murine cells. While animal models are important, they fail to replicate many aspects of human cardiac physiology, including beating rate and contractile protein composition. In this work, I used human induced pluripotent stem cells differentiated into CMs (hiPSC-CMs) to study the role of an adhesive interface mimicking cell-cell adhesion in human CMs. I seeded hiPSC-CMs onto patterns of N-cadherin, a protein critical for cell-cell adhesion in CMs. I used patterns with an elongated shape (7:1 aspect ratio and 1500 μm^2 area) to imitate the shape of mature human CMs. I did this patterning both on glass and on a polyacrylamide (PA) hydrogel at a physiologically relevant stiffness (~10 kPa), which imitates the native environment of mature human CMs. hiPSC-CMs adhered to N-cadherin patterns on glass, but not on PA hydrogels. I tested and ruled out several potential causes for the lack of adhesion on gels and propose future work to test other causes.

TABLE OF CONTENTS

LIST OF FIGURES

I. Introduction

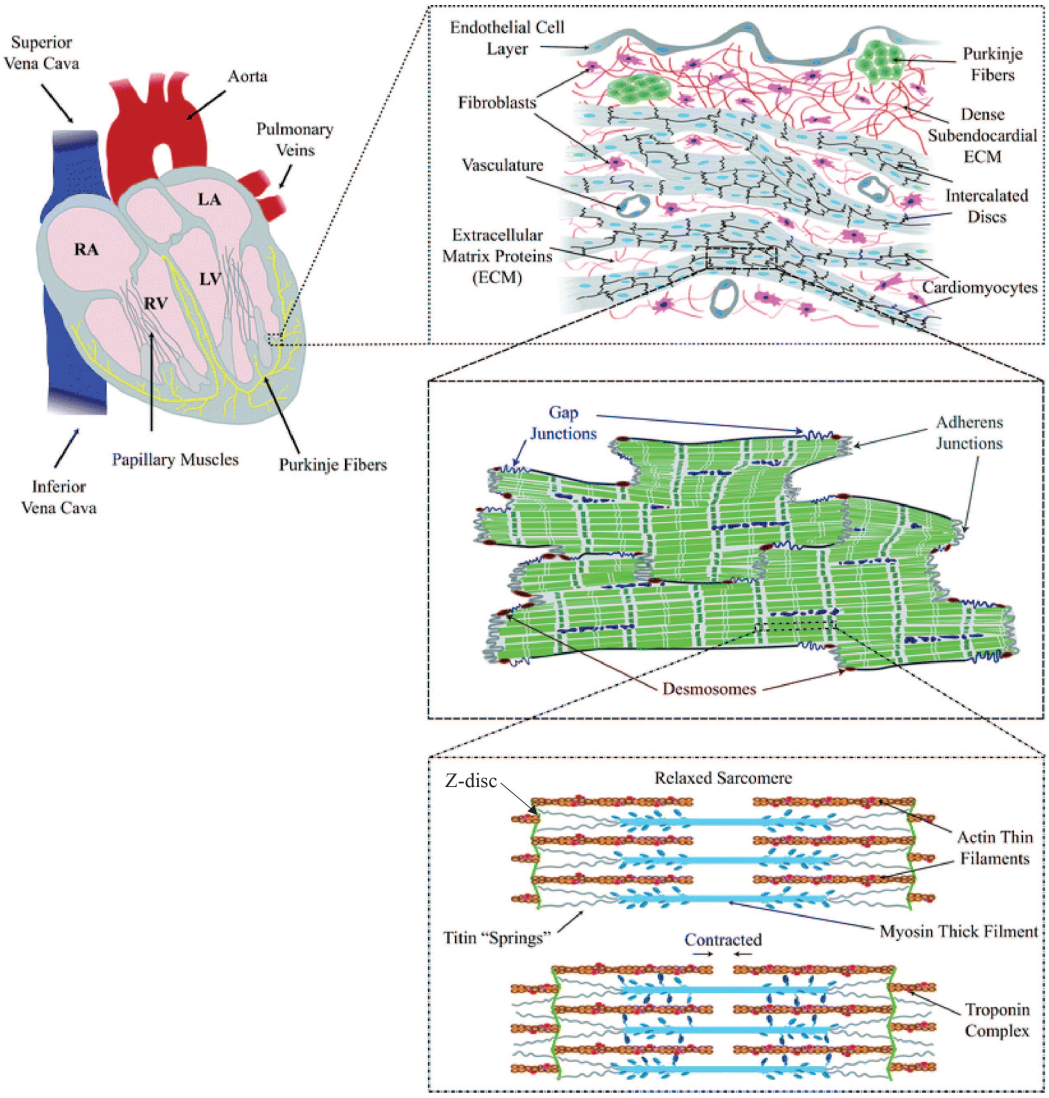

Figure 1. Schematics of (clockwise) heart, myocardium, cardiomyocytes and sarcomeres. Individual cardiomyocytes are distinguished by the adherens junctions, gap junctions, and desmosomes surrounding them. Abbreviations: RA = Right Atrium, LA = Left Atrium, RV = Right Ventricle, LV = Left Ventricle. Adapted from Simmons, et al.[1]

Heart disease is one of the leading causes of death in the world[2]. Research is needed to improve our understanding of the structure and function of the heart, causes of heart disease, and potential treatments. This research is generally limited to animal models, most often murine, because of the limited availability of human cardiomyocytes (CMs). CMs are the muscle cells of

the heart, comprised of force producing units called sarcomeres that join end-to-end with each other at intercalated discs (Figure 1). Sarcomeres contain the myosin motor proteins and actin filaments required for contractile movement and are joined together at the z-disc, where the actin thin filaments are bound[1]. In addition to this complex subcellular structure, CMs have a low regenerative capacity, turning over ~1% of cells per year at 25 years old and decreasing to ~0.45% by the age of 75[3]. Together, these factors restrict the availability of mature human CMs. Murine models are instructive but imperfect; there are many essential differences between murine and human heart morphology[4,5]. Rats have heart rates five times higher than humans and an inverse force to heart rate relationship[5]. In mature human CMs, about 95% of the sarcomeric myosin heavy chain (*MYH7*) is the beta isoform (*bMHC*)[6]. In murine models, the alpha isoform of *MYH7* (*aMHC*) is the predominant adult isoform[6,7]. These differences, along with others, demonstrate the need for a model that better imitates the human heart.

Human CMs are needed to bridge the gap between animal models and human disease. Fortunately, developments in cardiomyocyte differentiation protocols have expanded the use of human induced pluripotent stem cell-derived CMs (hiPSC-CMs)[8]. Induced pluripotent stem cells are differentiated cells that have been reprogrammed back to stemness[9,10]. These induced stem cells can then be differentiated into CMs (Figure 2). While this progress has been advantageous, there remain limitations to the use of hiPSC-CMs as models for mature human CMs. Primarily, there are critical differences in structure and function between hiPSC-CMs and mature human CMs[11]. One of the obvious differences between the two is morphology. Mature human CMs have an elongated shape with average length-to-width ratio of approximately 7 and highly aligned myofibrils. hiPSC-CMs are smaller and have an irregular shape and unaligned myofibrils, similar

to fetal human CMs[11,12]. Structural differences affect function, as is demonstrated by the impact of myofibril alignment on beating, indicating the importance of morphology in CM maturity[11,12].

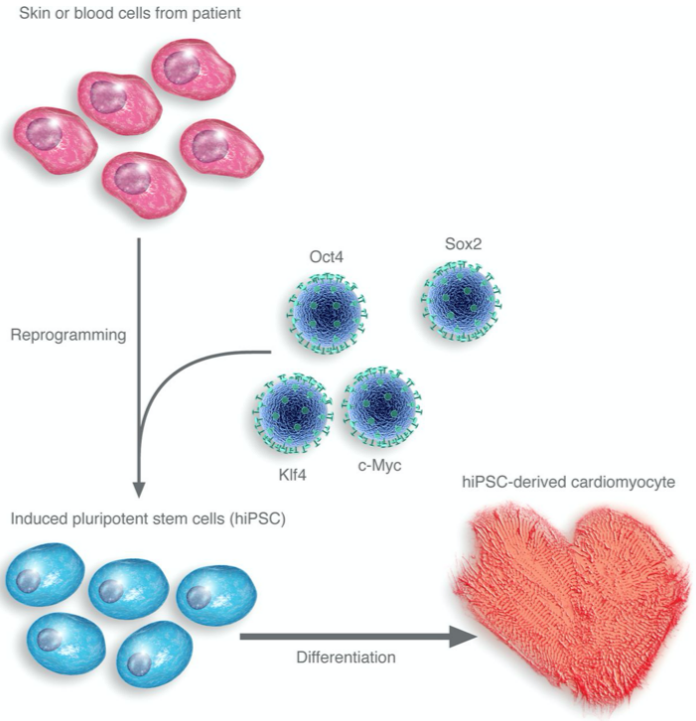

Figure 2. Schematic of flow from patient cell to hiPSC to hiPSC-CM. Reproduced from Eschenhagen, et al.[10]

One approach to improving hiPSC-CM maturity through morphology is by seeding them onto extracellular matrix (ECM) proteins patterned in aspect ratios similar to those of mature human CMs[12–14]. hiPSC-CM patterning is achieved by various methods[12–16], including isolating single CMs on rectangular protein patterns[12]. Patterned hiPSC-CMs present aligned myofibrils which produce higher contractile forces and other markers of maturity, such as calcium transient anisotropy[12]. This technique has been used with various device substrates, including polyacrylamide (PA) hydrogels[17].

PA hydrogels are commonly used due to their range of possible stiffnesses and their tunability. They are made up of crosslinked acrylamide monomers and adjusting the amount of monomer and crosslinker can change the stiffness and porosity of the resulting hydrogel[18,19]. The

possible stiffnesses of a PA hydrogel can range from approximately 1 kPa to 100 kPa, spanning a large range of physiological tissue stiffness[19].

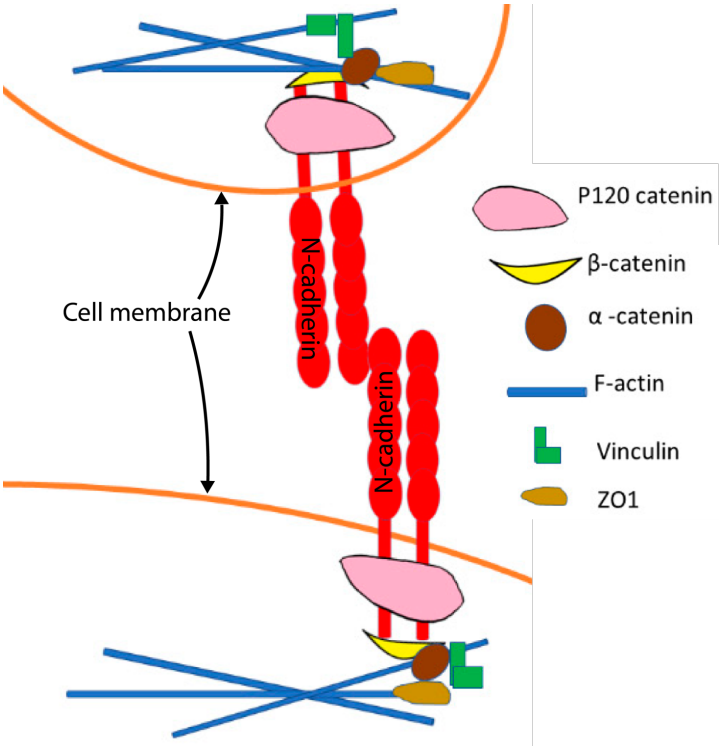

Figure 3. Schematic of an adherens junction. ZO1: zona occludens protein 1. Adapted from Loh, et al.[20]

Many studies have investigated how to make hiPSC-CMs resemble mature human CMs, including using cell patterning[11,12,21,22]. However, few studies have used cell patterning to look at the interactions between neighboring CMs and the effect this interplay has on hiPSC-CM maturity. Cell-cell interactions are crucial for force transmission between individual CMs in heart tissue, as well as communication between CMs. These interactions occur at intercalated discs, which contain three junction types, adherens junctions, desmosomes, and gap junctions. Adherens junctions link the actin cytoskeletons of adjoining cells (Figure 3), making them key players in intercellular force transmission. The fundamental binding protein in adherens junctions is N-cadherin[23].

For this work, I studied hiPSC-CM cell-cell interactions through N-cadherin attachment. I created single-cell-sized N-cadherin patterns on glass coverslips and PA hydrogels. I used PA hydrogels because of their physiologically relevant stiffness, which allows the PA to deform due to hiPSC-CM contraction. The deformation of PA provides an environment more similar to the native environment of cardiomyocytes and allows for measurement of the response of hiPSC-CMs acting against a load (the substrate). On glass substrates, hiPSC-CMs do not change length when contracting because glass is not deformable. Instead, hiPSC-CM contraction on glass is described as twitching[12,22,24]. By patterning N-cadherin on hydrogels, in the same manner done in previous studies with ECM proteins, I aimed to separate the effects of cell-cell interactions from those of cell-ECM interactions to explore the impact of cell-cell junctions on morphology and force generation in hiPSC-CMs.

II. Methods

A. Cell Culture and Differentiation

In this work, I used human induced pluripotent stem cells (hiPSCs) modified with a GFP fluorophore marking α-actinin[25,26] (Coriell, AICS-0075-085) (α-act-hiPSCs). α-actinin is a protein that facilitates actin crosslinking within the z-disc[27]. α-act-hiPSCs were chosen for this work because z-discs, and α-actinin within the z-disc, should be present in the sarcomeres of differentiated CMs and not in hiPSCs[25]. α-act-hiPSC-differentiated CMs (α-act-hiPSC-CMs) allow me to screen cells on devices and select only those which have differentiated to CMs based on their GFP expression. α-act-hiPSC-CMs also provide visualization of sarcomere structure in hiPSC-CMs without the need to fix and stain samples. Sarcomere alignment is one of the features commonly used for determining maturity of hiPSC-CMs[6].

I differentiated α-act-hiPSCs into CMs using a previously published protocol[28]. hiPSCs were cultured in Essential 8 Medium (ThermoFisher) preceding differentiation. Essential 8 Medium is a xeno-free medium designed for culturing human pluripotent stem cells and maintaining pluripotency (ThermoFisher). Three days before differentiation, I passaged the hiPSCs onto a plate coated in Matrigel Basement Membrane Matrix (Matrigel, Corning) diluted 1:30 in Dulbecco's Modified Eagle Medium: Nutrient Mixture F-12 (DMEM/F12, ThermoFisher). Matrigel is a basement membrane-derived protein cocktail commonly used for substrate attachment and differentiation of mammalian cells (Corning). DMEM/F12 is a medium commonly used for mammalian cell culture (ThermoFisher). On day 0, I gave the hiPSCs RPMI 1640 Medium with B27 minus insulin supplement (B27-INS, ThermoFisher) with 6 μM CHIR-99021 (SelleckChem). B27-INS is a serum-free medium supplement that supports the growth of hiPSC-CMs in an insulin-free environment[9,28] (ThermoFisher). CHIR-99021 is a GSK3-β inhibitor that induces mesodermal differentiation[9,28]. After two days, I changed the media to B27-INS with 2 μM Wnt-C59 (SelleckChem). Wnt-C59 is a Wnt pathway inhibitor that initiates cardiac differentiation[9,28]. Wnt has been recognized as a critical pathway for cardiac differentiation[9]. After another two days, I changed the media to B27-INS. After two days, I changed the media to RPMI 1640 Medium with B27 supplement (B27, ThermoFisher). B27 is a serum-free medium that supports maintenance of hiPSC-CMs[28]. I changed the media to fresh B27 every two days until the onset of beating. After the onset of beating, which occurs at approximately day 10, I changed the media to RPMI 1640 Medium, no Glucose with B27 supplement (B27-glucose, ThermoFisher). B27-glucose is a serum-free medium that is used for purification of hiPSC-CMs via glucose starvation. Glucose starvation removes non-cardiomyocytes from the hiPSC-CM monolayer because CMs can survive off of lactate, which is

present in B27-glucose, but non-cardiomyocytes cannot[28]. I changed the media to fresh B27-glucose every 2 days for 4 days, at which point I returned the media to B27. I changed the media every two days to fresh B27 for the rest of culture, typically 20 days total. I seeded hiPSC-CMs on devices approximately 20 days after the addition of CHIR-99021, consistent with the age of stem cell-derived CMs commonly used in studies[29–32].

B. Protein Patterning

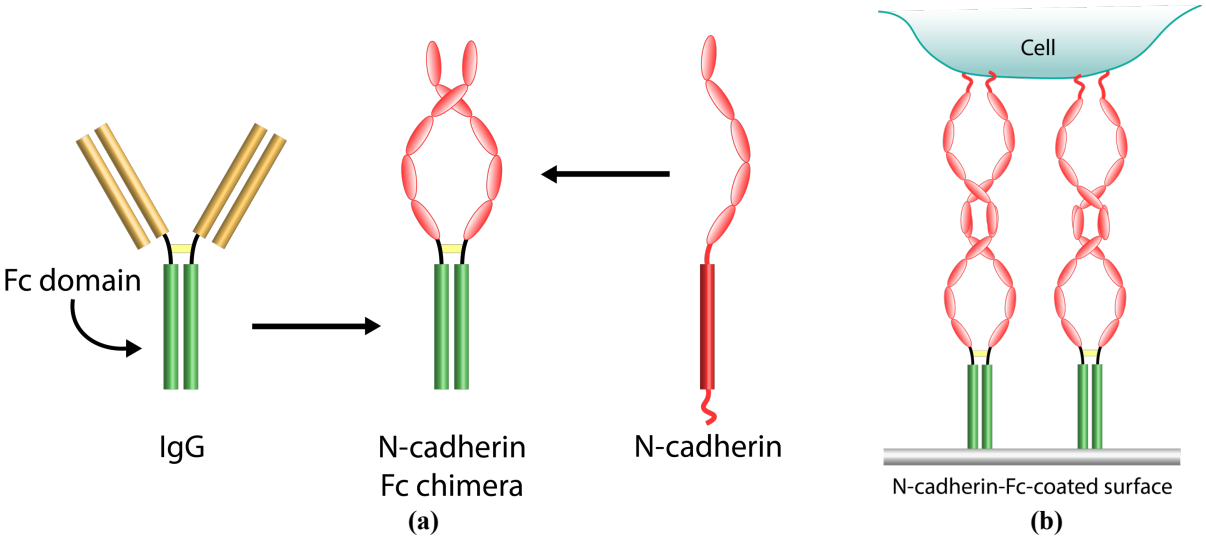

Figure 4. (a) Structure of an N-cadherin Fc chimera. **(b)** Schematic of N-cadherin Fc chimera-functionalized surface attaching a cell. Adapted from Nag, et al.[33]

For this work, I used an N-cadherin Fc chimera (R&D Systems). This chimera protein is a combination of the extracellular domain of N-cadherin and the Fc region of IgG[34] (Figure 4). The Fc region allows for attachment of N-cadherin to a substrate via a linker protein and ensures the extracellular binding domain is available for cell attachment[34,35]. In this work, I used Protein A (Sigma), a protein known for binding to the Fc domain of immunoglobulin proteins[34,35], as a linker.

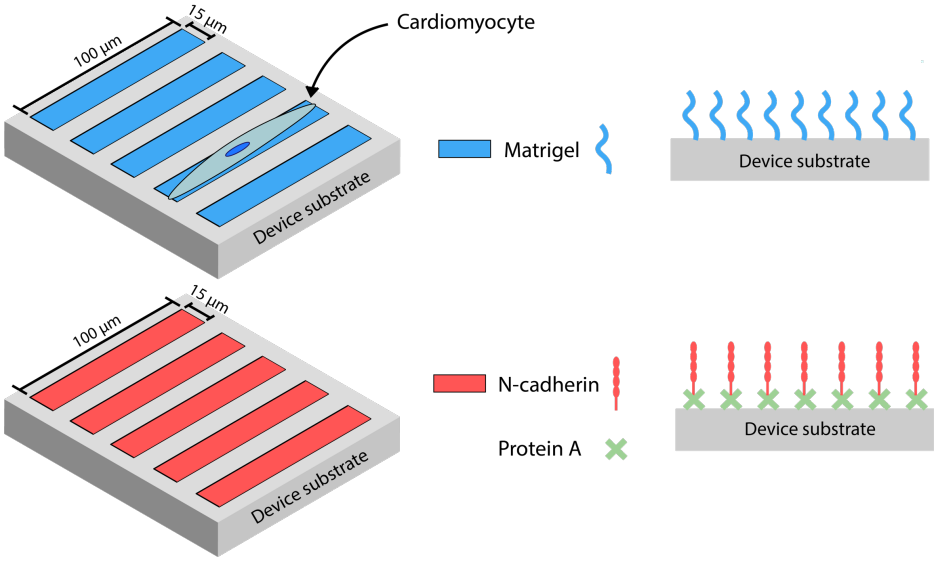

Figure 5. Schematic of N-cadherin and Matrigel devices.

I made both N-cadherin and Matrigel patterned devices to replicate cell-cell and cell-ECM interactions, respectively (Figure 5). I made protein patterns using lift-off, a previously published technique for fabricating protein patterns[14]. I used lift-off because it produces high repeatable patterns[14].

I patterned glass coverslips with AZ1512 photoresist (MicroChemicals) via photolithography (Figure 6a). Next, I incubated photoresist-patterned coverslips with poly(L-lysine)-g-poly(ethylene glycol) (PLL-g-PEG, SuSoS) at a concentration of 6 µg/cm^2. PLL-g-PEG is a protein frequently used to prevent non-specific binding[14,36]. Then, I removed the photoresist patterns from the coverslips with N-methyl-2-pyrrolidone (EMD Performance Materials), leaving behind Pll-g-PEG in the inverse pattern on the coverslip. Finally, I added the protein of interest to the coverslips (Figure 6b). For N-cadherin devices, I incubated Protein A at a concentration of 6 µg/cm^2 for 4 hours at 4ºC. For Matrigel devices, I incubated Matrigel at a 1:10 dilution of stock for 4 hours at 4ºC.

For glass devices, I incubated the Protein A-patterned coverslips with human recombinant N-cadherin (R&D Systems) at a concentration of 3 µg/ cm^2 for 3 hours at 4ºC and subsequently stored in phosphate buffered saline (PBS, ThermoFisher) at 4ºC until cell seeding.

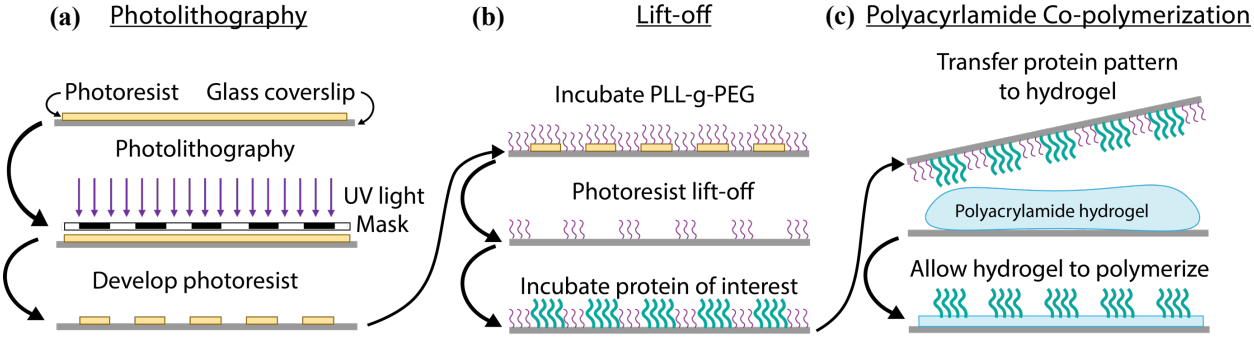

Figure 6. Process flow for creating protein-patterned PA hydrogels: **(a)** photolithography, **(b)** liftoff, **(c)** and PA polymerization and protein transfer. Adapted from Moeller et al.[14].

C. Polyacrylamide Hydrogel Fabrication

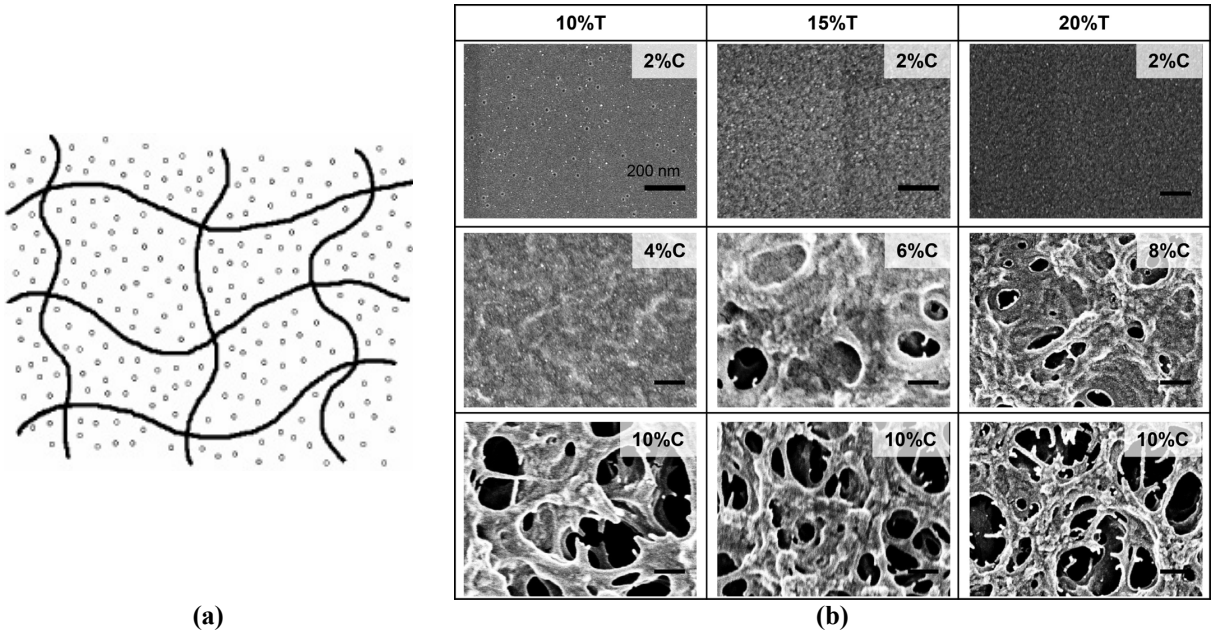

Figure 7. (a) Schematic of a swollen PA network where the black lines represent the acrylamide monomers and the white space with grey dots indicate solvent. **(b)** SEM images of PA hydrogels with varying monomer and crosslinker concentrations. Scale bar is 200 nm. Adapted and reproduced from Di Benedetto, et al.[37] and Denisin, et al.[19], respectively.

PA hydrogels are commonly used for hiPSC-CM patterning because of their tunable stiffness and linear elastic behavior[19]. PA hydrogels consist of acrylamide monomers crosslinked by bisacrylamide (Figure 7). The stiffness and porosity can be adjusted by changing the concentration of bisacrylamide and acrylamide[18,19]. Most studies define PA hydrogels by two figures, total polymer content (*%T*) and cross-linker concentration (*%C*), which are defined in equations (1) and (2).

$$\%T = \frac{\text{acrylamide (g)+bisacrylamide (g)}}{\text{total volume (mL)}} \times 100\% \quad (1)$$

$$\%C = \frac{\text{bisacrylamide (g)}}{\text{acrylamide (g)+bisacrylamide (g)}} \times 100\% \quad (2)$$

For this work, I used 10%T, 1%C PA hydrogels, which have a stiffness of about 10 kPa[19]. A stiffness of 10 kPa allows the PA hydrogel to deform in response to hiPSC-CM contractile force[38], making these PA hydrogels suitable for measuring the force hiPSC-CMs produce during contraction. 10 kPa is also near the physiological stiffness of adult human heart tissue[11], making these 10 kPa PA hydrogels good replicators of the native environment of CMs.

I made polyacrylamide (PA) hydrogels following a previously established protocol[19]. I treated glass bottom dishes (#1.5, Cellvis) with 3-(trimethoxysilyl)propyl methacrylate (bind-silane, Sigma) to secure the bottom of the PA hydrogel to the glass dish. I coated the dishes with a 0.3% bind-silane solution in ethanol (Spectrum) and 5% glacial acetic acid (Spectrum) for 10 minutes, then rinsed them with ethanol, and finally dried them with N_2 gas. I mixed prepolymer solutions containing acrylamide (Sigma), bisacrylamide (Sigma), HEPES (ThermoFisher), ammonium persulfate (Sigma), N,N,N′,N′-tetramethylethylenediamine (Sigma), fluorescent microbeads (diameter 0.5 μm, ThermoFisher), and MilliQ water. I pipetted 50 μL of the polyacrylamide solution onto a bind-silane-treated glass-bottom dish, sandwiched it with a N-

cadherin-patterned glass coverslip (Figure 6c), and left it to polymerize for 30 minutes at room temperature.

After 30 minutes of polymerization, I flooded the PA hydrogels with PBS and left them to polymerize further overnight. Then, I removed the top coverslip and washed the hydrogels three times with PBS. I stored the Matrigel hydrogels at 4ºC until cell seeding. I incubated the Protein A hydrogels with N-cadherin at a concentration of 3 μg/ cm^2 for 3 hours at 4ºC. After N-cadherin incubation, all devices were seeded with hiPSC-CMs at the same time. N-cadherin patterns were verified with anti-rabbit-pan-cadherin antibody (Sigma) and AlexaFluor 488 polyclonal antibody (AF488, ThermoFisher).

D. Cell Seeding

After fabricating the devices described above, I seeded them with hiPSC-derived CMs (hiPSC-CMs) at a density of 10,000 cells/cm^2. I lifted up hiPSC-CMs from their monolayer using TrypLE 10X (ThermoFisher) for 5 to 10 minutes at 37ºC. TrypLE is a cell-dissociation reagent containing animal-free recombinant enzymes to replace animal-derived trypsin (ThermoFisher). After incubating the hiPSC-CMs in TrypLE, I diluted the TrypLE by adding B27 media with 1% Penicillin-Streptomycin (Pen-Strep, ThermoFisher) and 10 μM Y-27632 (SelleckChem) (B27+P/S+Y). Pen-Strep is an antibiotic solution commonly used in mammalian cell culture to prevent bacterial contamination (ThermoFisher). Y-27632 is a ROCK inhibitor that prevents apoptosis[39] and enhances survival of hiPSC and hiPSC-CMs after passaging[28]. I collected the resulting solution in a 15 mL conical tube, which I spun in a centrifuge at 200 x g for 3 to 5 minutes, until a pellet formed at the bottom of the tube. I aspirated the supernatant and resuspended the cells in fresh B27+P/S+Y. I stained a sample of the resuspended cells with Trypan Blue (ThermoFisher) and counted cells on a hemocytometer to achieve the desired

density of 10,000 cells per device. Trypan Blue is a commonly used cell viability stain that dyes dead cells exclusively. Then, I flooded the devices with the resuspended cell solution and left them in the incubator at 37ºC for 48 hours. After 48 hours, I changed the media in the devices to B27 with 1% Pen-Strep every two days. I imaged the devices on a widefield fluorescent microscope between 3 and 5 days after seeding.

III. Results

A. N-cadherin Was Successfully Patterned on Glass and PA Hydrogel Substrates

To study the effect of cell-cell interactions on hiPSC-CM maturity, I aimed to isolate cell-cell contacts from cell-ECM contacts. To do this while still maintaining the elongated morphology previously studied, I made rectangular N-cadherin patterns with an area of 1500 μm^2 and an aspect ratio of 7:1 on glass coverslips and PA hydrogels (Figure 8). The 7:1 aspect ratio was chosen because it had been shown in a previous study to induce a more mature phenotype in stem cell-derived CMs[12]. The 1500 μm^2 area was chosen because cells failed to fill the 2000 μm^2 patterns reported in the previous study.

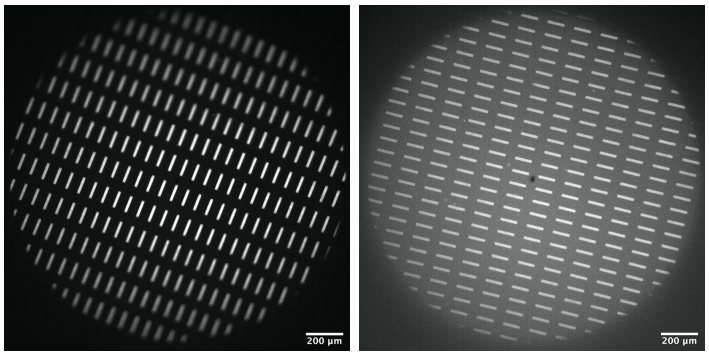

(a) **(b)**

Figure 8. Fluorescence images of patterned N-cadherin on **(a)** glass and **(b)** hydrogel devices using liftoff and visualized with pan-cadherin primary antibody and AF488 secondary antibody.

To demonstrate the presence of N-cadherin on the devices, I performed immunostaining with a pan-cadherin antibody. Pan-cadherin is an antibody that can bind to any of the cadherin

proteins, including N-cadherin. This verified the presence of N-cadherin on both glass and PA hydrogel surfaces (Figure 8).

To further confirm the presence of N-cadherin, I tested the specificity of the antibodies. To demonstrate the pan-cadherin antibody did not bind non-specifically to the substrate, I stained lift-off-patterned coverslips not incubated in protein with the pan-cadherin antibody and then the AF488 antibody (Figure 9a). To show that the AF488 antibody was not binding non-specifically to the substrate, I stained patterned coverslips not incubated in protein with the AF488 antibody only (Figure 9b).

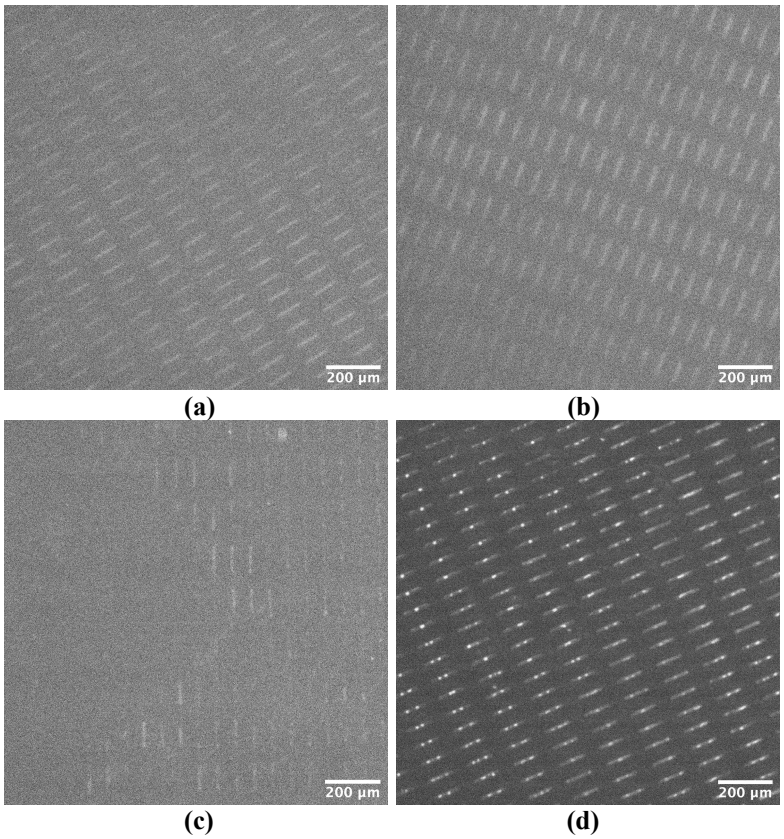

Figure 9. Fluorescence images of immunostaining controls: **(a)** no protein devices stained with pan-cadherin and AF488 antibodies, **(b)** no protein devices stained with AF488 antibody, **(c)** devices patterned with laminin stained with pan-cadherin and AF488 antibodies, and **(d)** devices patterned with Protein A stained with pan-cadherin and AF488 antibodies.

To check that the pan-cadherin antibody did not bind non-specifically to other proteins, I incubated lift-off-patterned coverslips in laminin, an ECM protein, and then stained with pan-cadherin and AF488 (Figure 9c). Finally, I stained devices incubated in only Protein A to determine if the pan-cadherin antibody could bind to the N-cadherin-binding region of Protein A (Figure 9d). I used patterned glass instead of patterned gels for these tests because it decreased the time and materials necessary. I justified this because, in general, proteins are more inclined to bind to a glass surface than a PA hydrogel surface, which naturally inhibits protein and cell binding[13,16].

B. hiPSC-CMs Attach to N-cadherin Patterns on Glass Coverslips

After verifying N-cadherin patterning, I seeded hiPSC-CMs on devices. For each experiment I made N-cadherin-patterned PA hydrogels and Matrigel-patterned PA hydrogels, as well as N-cadherin-patterned glass coverslips and Matrigel-patterned glass coverslips to control for substrate. The Matrigel hydrogels served as cell-seeding controls, as cells attach robustly to Matrigel[6,12,38].

I seeded α-act-hiPSC-CMs on all four device types: N-cadherin on glass, N-cadherin on hydrogel, Matrigel on glass, and Matrigel on hydrogel. α-act-hiPSC-CMs allow for screening the CMs on the devices and provide live sarcomere visualization. I can get information about the maturity of hiPSC-CMs by visualizing sarcomeres. Following seeding, I saw successful hiPSC-CM attachment and patterning on Matrigel on glass, Matrigel on hydrogel, and N-cadherin on glass (Figure 10).

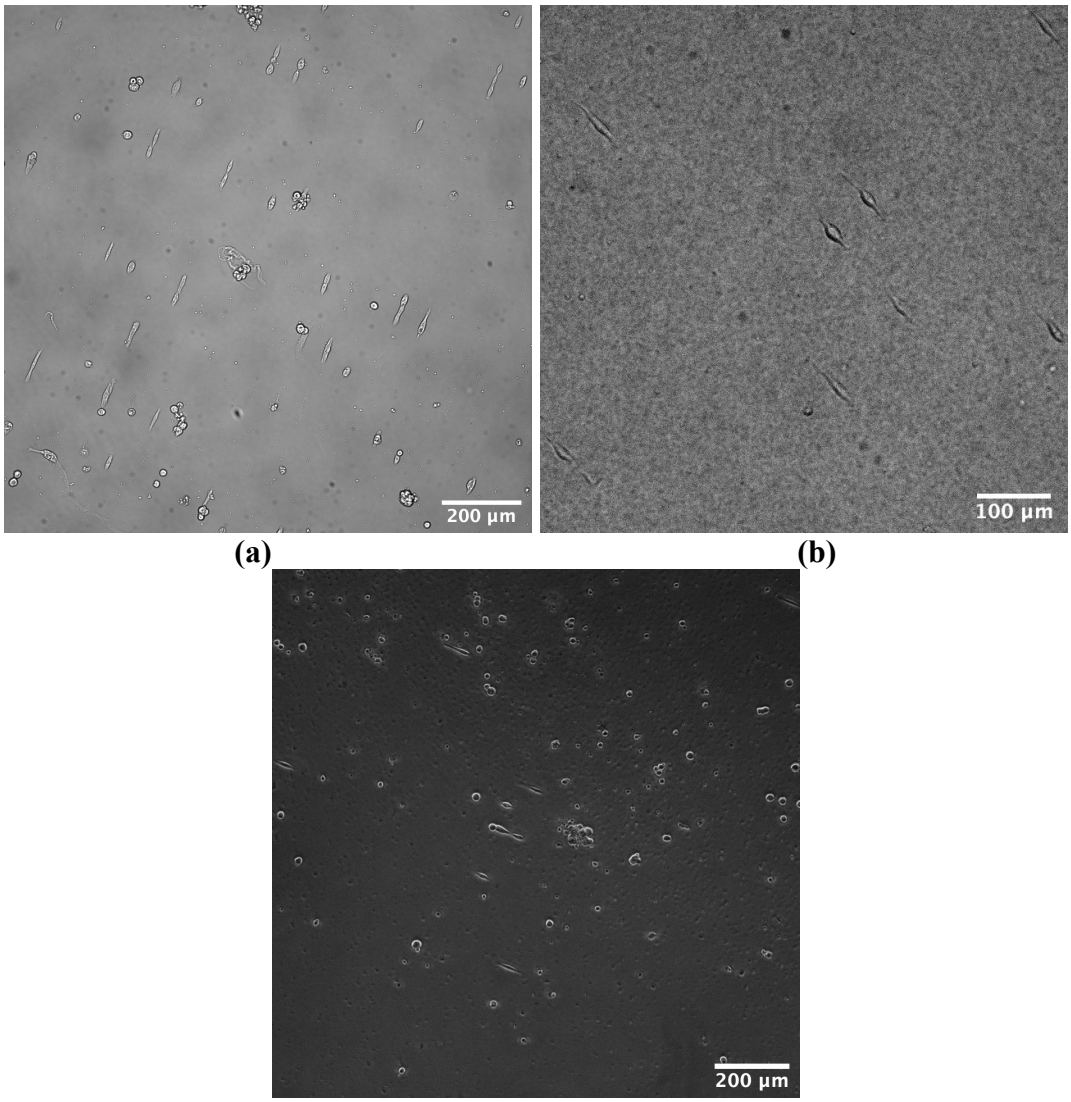

(a) **(b)**

(c)

Figure 10. Brightfield images of α-actinin-tagged hiPSC-CMs seeded on **(a)** Matrigel on glass, **(b)** Matrigel on hydrogel, and **(c)** N-cadherin on glass devices.

I verified that hiPSC-CM seeding was successful by cell beating and GFP signal at z-discs, which can be visualized clearly with a Matrigel on PA hydrogel device in Figure 11. The presence of z-discs' indicates that the imaged cells were hiPSC-CMs and not fibroblasts[25]. I did not acquire high-quality GFP images of N-cadherin on glass devices, so further imaging will be necessary to better demonstrate the presence of hiPSC-CMs via GFP signal.

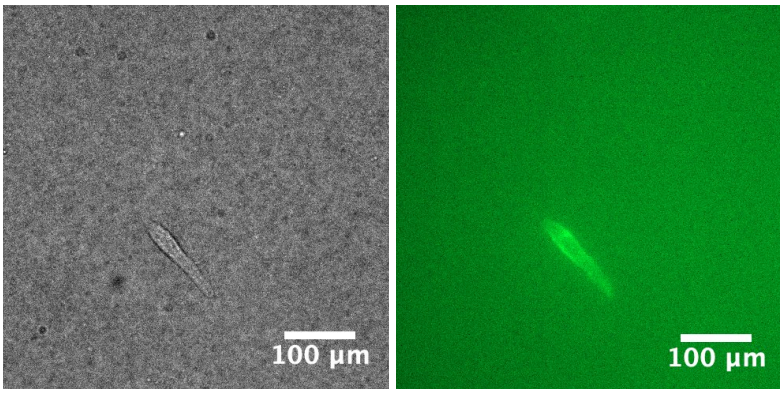

(a) **(b)**

Figure 11. α-actinin-tagged hiPSC-CMs seeded on Matrigel on hydrogel and visualized with **(a)** brightfield and **(b)** fluorescence microscopy.

C. hiPSC-CMs Displayed Elongated Morphology on N-cadherin-Patterned Glass

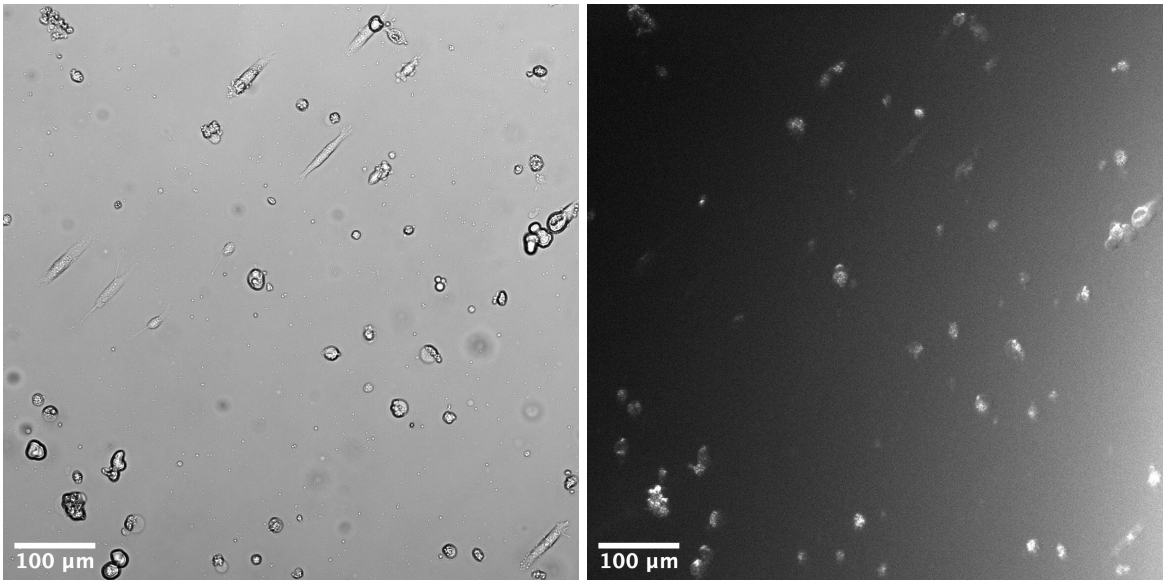

(a) **(b)**

Figure 12. α-actinin-tagged hiPSC-CMs seeded on N-cadherin on glass devices and visualized with **(a)** brightfield and **(b)** fluorescence microscopy.

As can be seen in Figure 12, the hiPSC-CMs on N-cadherin patterns demonstrated elongated morphology indicating increased maturity. In addition to verifying hiPSC-CM attachment, further imaging will be necessary to establish z-disc alignment on the N-cadherin on glass devices. The GFP image seen in Figure 12 shows the presence of GFP signal in the

patterned cells but background fluorescence from cell debris washes out much of the signal. Also, higher magnification images will allow for better visualization of individual sarcomeres, which will better indicate the level of alignment of the sarcomeres within the patterned hiPSC-CM.

D. hiPSC-CMs Did Not Attach to N-cadherin-Patterned PA Hydrogels

Although I saw hiPSC-CM attachment on N-cadherin on glass devices, I did not see attachment on N-cadherin on hydrogel devices (Figure 13).

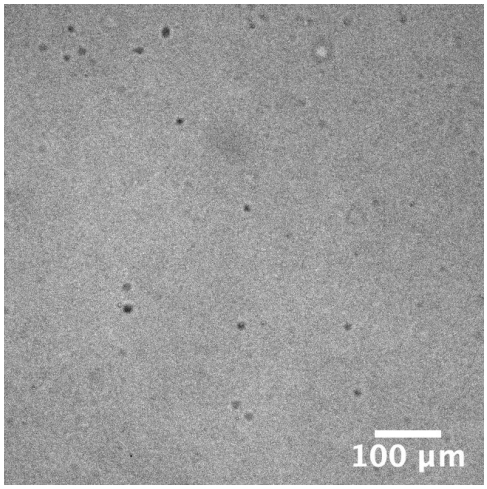

Figure 13. Brightfield image of α-actinin-tagged hiPSC-CMs seeded on N-cadherin on hydrogel device.

To examine the impact of patterning on cell attachment to N-cadherin, I made unpatterned N-cadherin devices, with N-cadherin covering the entire surface, on both glass and PA hydrogels. These devices were made following the same protocol as the patterned devices, without the photolithography and liftoff processes.

hiPSC-CMs attached readily to the unpatterned N-cadherin on glass devices and resumed beating. Because they are not patterned, these hiPSC-CMs demonstrated a more immature phenotype, specifically in their rounded morphology. Like the patterned N-cadherin, no cells attached to the unpatterned N-cadherin on hydrogel devices (Figure 14).

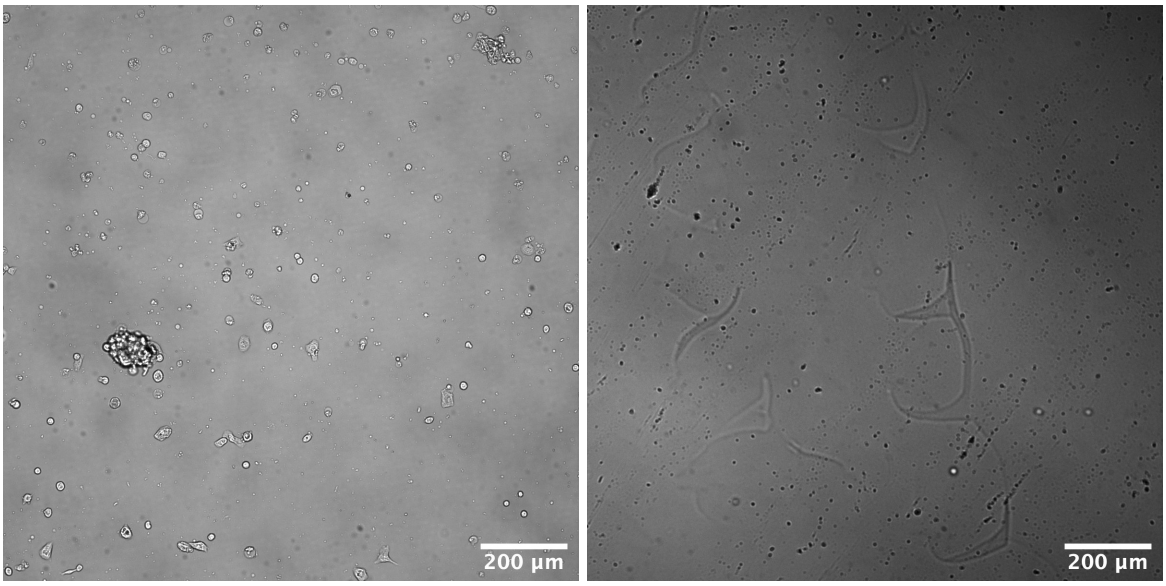

(a) **(b)**

Figure 14. Brightfield images of hiPSC-CMs seeded on unpatterned **(a)** N-cadherin on glass and **(b)** N-cadherin on hydrogel devices.

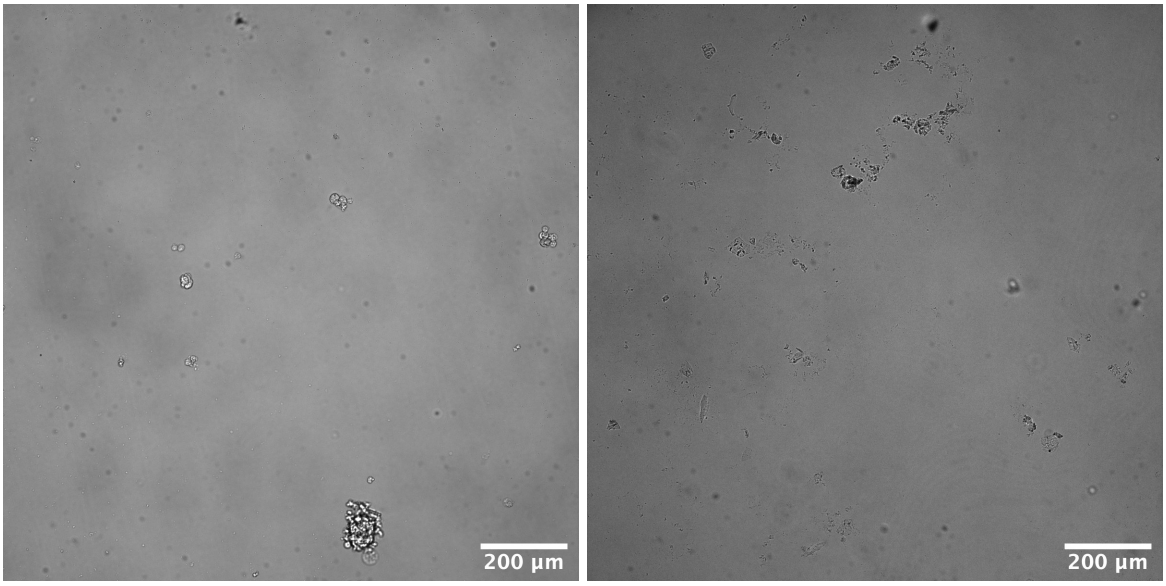

(a) **(b)**

Figure 15. Brightfield images of hiPSC-CMs seeded on **(a)** glass and **(b)** hydrogel devices not functionalized with protein.

To determine whether cells adhere specifically to N-cadherin on glass, and to test the non-binding quality of PA hydrogels, I made glass and PA hydrogel devices without any protein functionalized to the surfaces. The glass devices without protein had some debris adhesion, but

no single CM attachment or beating (Figure 15a). The PA hydrogel devices without protein had no attachment at all (Figure 15b).

Because hiPSC-CMs attach to N-cadherin on glass, I speculated that the lack of cells on N-cadherin on PA hydrogel devices was due to the inability of the PA hydrogel to anchor N-cadherin its surface. To determine if N-cadherin was still present on the PA hydrogel surface after hiPSC-CM seeding and a lack of attachment, I stained previously seeded N-cadherin patterned PA hydrogels with pan-cadherin and AF488 (Figure 16). All N-cadherin patterns had been removed from the hydrogel surface, indicating that N-cadherin is degraded or removed in the process of hiPSC-CM seeding.

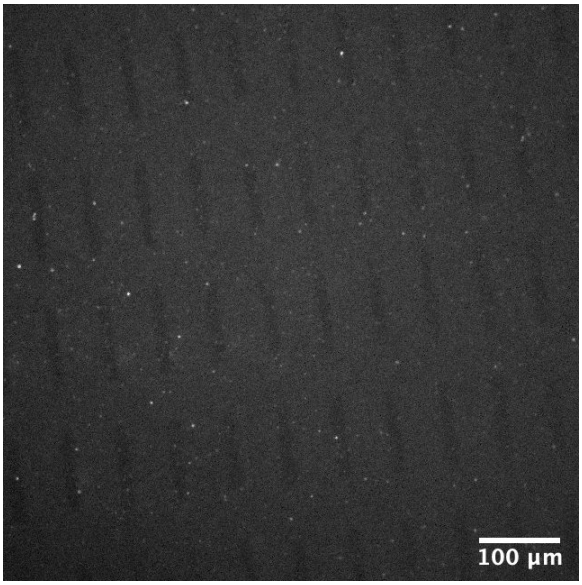

Figure 16. Fluorescence image of a patterned N-cadherin on hydrogel device after hiPSC-CM seeding and lack of attachment. Device was immunostained with pan-cadherin and AF488 antibodies.

To demonstrate that the degradation or removal of N-cadherin is not due to the time elapsed between incubation and staining, I made three patterned N-cadherin on hydrogel devices at the same time as the one I seeded. I stained and imaged them at successive time points. The first was stained and imaged the day of seeding (Figure 17a), the second two days after seeding

(Figure 17b), and the third three days after seeding (Figure 17c). The seeded device that failed to attach cells was also stained and imaged three days after seeding. With the unseeded devices, there was slight degradation of N-cadherin pattern with time, but overall the pattern was preserved.

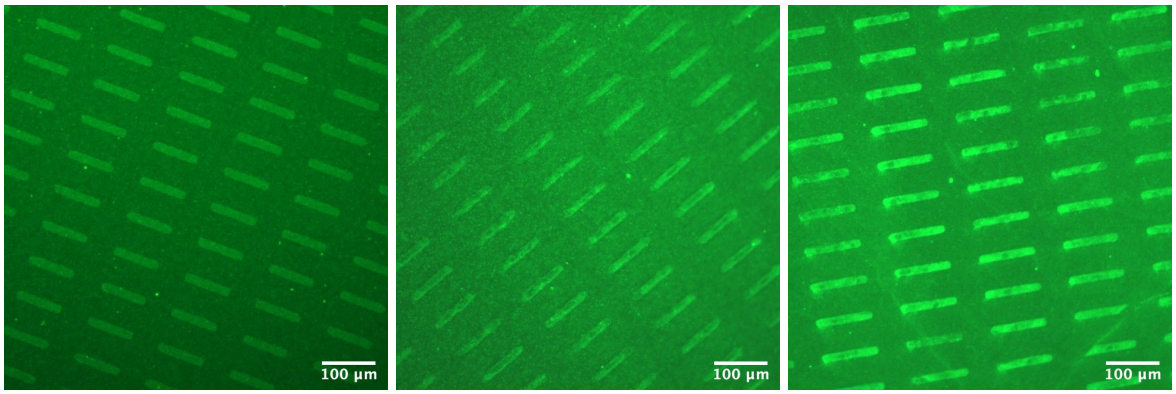

(a) **(b)** **(c)**

Figure 17. GFP images of N-cadherin patterned on hydrogel devices immunostained **(a)** the day of seeding, **(b)** two days after seeding, and **(c)** three days after seeding. Patterns were visualized with pan-cadherin primary antibody and AF488 secondary antibody.

IV. Discussion

As was shown in the results, N-cadherin can be patterned via lift-off on both glass coverslips and PA hydrogels, but hiPSC-CMs can adhere only to N-cadherin patterns on glass coverslips. This result is promising for future studies of cell-cell interactions between hiPSC-CMs and the impact of cell-cell adhesion on hiPSC-CM maturity. Future work can use this platform to determine if any differences in structure or function occur between hiPSC-CMs patterned on Matrigel or N-cadherin on glass devices.

Between Matrigel and N-cadherin patterned glass devices, there was far higher cell attachment on Matrigel than on N-cadherin. This is unsurprising given that cells attached to Matrigel hydrogels but not N-cadherin hydrogels. Also, there was more debris or non-specific

cell attachment on N-cadherin patterned glass devices than on Matrigel patterned glass devices. The amount of debris or non-specific cell attachment on the N-cadherin patterned glass devices is greater than was seen on the no-protein glass controls. This might be due to the cells attached to the N-cadherin patterns laying down their own ECM proteins which other cells can non-specifically bind to. It could also be cells that attached to N-cadherin weakly and were therefore not restrained by the N-cadherin pattern. In this case, weak bonds could be broken after the cell laid down their own ECM proteins. This hypothesis would explain the N-cadherin removal from PA hydrogels, as well. I saw no remaining N-cadherin patterns after hiPSC-CM seeding, which would fit with the hypothesis that hiPSC-CMs attached to patterns and then broke the bonds between the protein and the substrate.

The inability of N-cadherin copolymerized to PA hydrogels to anchor hiPSC-CMs is consistent with previous work done with E-cadherin and Madin-Darby Canine Kidney (MDCK) cells by a previous member of the Pruitt Lab[40]. In this previous work, MDCK cells were successfully cultured on PA hydrogels that were functionalized with E-cadherin via Protein A and a chemical linker, sulfosuccinimidyl 6-[40-azido-20-nitro-phenylamino]hexanoate (Sulfo-SANPAH) [40,41]. The E-cadherin was coated uniformly across the entire PA hydrogel surface, not patterned. PA hydrogels patterned with Protein A via lift-off, which cannot be used with Sulfo-SANPAH, and then E-cadherin, did not successfully adhere and constrain the MDCK cells[40].

I have a few hypotheses that would be interesting to explore in the future. One hypothesis for the lack of adhesion is that the pores of the 10%T, 1%C PA hydrogel are too large relative to the size of Protein A. Therefore, Protein A, and thus N-cadherin, is not strongly attached to the PA hydrogel surface when copolymerized. This hypothesis is difficult to test, as the mechanism for copolymerization is not fully understood[19]. However, one method to probe this hypothesis

would be to compare various formulations for PA hydrogels with the same stiffness (about 10 kPa), as well as PA hydrogels with various stiffnesses. If a 10 kPa PA hydrogel with higher crosslinker concentration, for example 8%T, 5%C, can anchor Protein A and N-cadherin during hiPSC-CM attachment, it would indicate that the PA hydrogel structure participated in the lack of hiPSC-CM attachment to the patterned N-cadherin on PA hydrogel devices. If a stiffer hydrogel can anchor protein A and N-cadherin during hiPSC-CM attachment, it would indicate that higher stiffness is required for stable binding.

If changing the structure of the PA hydrogel does not allow for hiPSC-CM attachment to N-cadherin patterns, then another approach to increase the strength of attachment, such as using a covalent linker between the PA hydrogel surface and Protein A, is necessary. In the previous study with E-cadherin and MDCK cells, Sulfo-SANPAH was used to covalently bind the Protein A to the hydrogel surface[40]. Other linkers have been used in previous studies, including N-hydroxyethylacrylamide (HEA)[15]. Either of these linkers would be good options for adhering Protein A to a PA hydrogel surface, however neither have been previously reported with the lift-off method. Sulfo-SANPAH is not compatible with lift-off, so it would be necessary to use another protein patterning technique. HEA might be compatible with lift-off, but a protocol for HEA with lift-off has not yet been reported.

If Protein A is covalently attached to a PA hydrogel and N-cadherin still cannot anchor hiPSC-CMs, it is likely that either N-cadherin itself or the contact between N-cadherin and Protein A cannot sustain the loading from hiPSC-CMs on PA hydrogel devices. Previous studies have shown that CM contraction on glass is distinct from on Matrigel- and fibronectin-coated PA hydrogels, with PA hydrogels allowing CMs to fully contract. On glass, CMs are unable to change their overall length while contracting, so instead they move in a twitching fashion[12,22,24].

This difference in force generation could create loading that is above the threshold of what N-cadherin or the N-cadherin-Protein A bond can tolerate. This threshold for N-cadherin is hard to estimate because N-cadherin does not have to mediate cell forces without cell-ECM interactions for stabilization in the native environment. Therefore, to test whether the N-cadherin-Protein A bond can tolerate the loading produced by cell attachment, I could do an AFM rupture test to determine the force required to pull apart Protein A and N-cadherin.

If it is not possible to stably attach N-cadherin to PA hydrogels, it will be difficult to attach cells without the assistance of ECM proteins. In this case, I could transition my approach from trying to isolate to cell-cell interactions to studying cell-cell interactions with cell-ECM attachments to stabilize the cells. Replicating cell-cell and cell-ECM interactions could be achieved by patterning both Matrigel and N-cadherin in a given pattern (Figure 18).

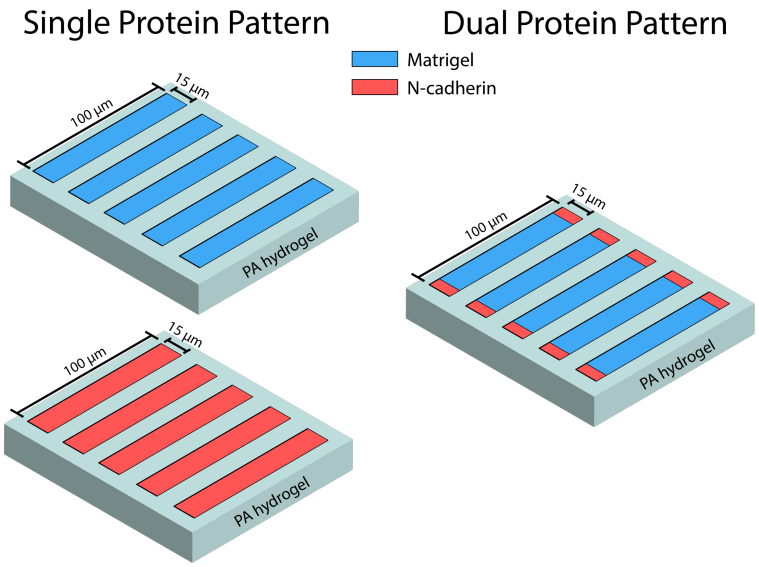

Figure 18. Schematics of single and dual protein patterns**.**

References

1. Simmons, C. S., Petzold, B. C. & Pruitt, B. L. Microsystems for biomimetic stimulation of cardiac cells. *Lab Chip* **12**, 3235–3248 (2012).
2. Benjamin, E. J. *et al.* Heart Disease and Stroke Statistics-2019 Update: A Report From the American Heart Association. *Circulation* **139**, e56–e528 (2019).
3. Bergmann, O. *et al.* Evidence for cardiomyocyte renewal in humans. *Science (80-.).* **324**, 98–102 (2009).
4. Milani-Nejad, N. & Janssen, P. M. L. Small and large animal models in cardiac contraction research: Advantages and disadvantages. *Pharmacology and Therapeutics* vol. 141 235–249 (2014).
5. Hasenfuss, G. Animal models of human cardiovascular disease, heart failure and hypertrophy. *Cardiovascular Research* vol. 39 60–76 (1998).
6. Schroer, A., Pardon, G., Castillo, E., Blair, C. & Pruitt, B. Engineering hiPSC cardiomyocyte in vitro model systems for functional and structural assessment. *Prog. Biophys. Mol. Biol.* **144**, 3–15 (2019).
7. Weiss, A. & Leinwand, L. A. THE MAMMALIAN MYOSIN HEAVY CHAIN GENE FAMILY. *Annu. Rev. Cell Dev. Biol.* **12**, 417–439 (1996).
8. Zhang, J. *et al.* Functional cardiomyocytes derived from human induced pluripotent stem cells. *Circ. Res.* **104**, (2009).
9. Burridge, P. W. *et al.* Chemically defined generation of human cardiomyocytes. *Nat. Methods* **11**, 855–860 (2014).
10. Eschenhagen, T., Mummery, C. & Knollmann, B. C. Modelling sarcomeric cardiomyopathies in the dish: From human heart samples to iPSC cardiomyocytes.

Cardiovasc. Res. **105**, 424–438 (2015).

11. Yang, X., Pabon, L. & Murry, C. E. Engineering adolescence: Maturation of human pluripotent stem cell-derived cardiomyocytes. *Circ. Res.* **114**, 511–523 (2014).
12. Ribeiro, A. J. S. *et al.* Contractility of single cardiomyocytes differentiated from pluripotent stem cells depends on physiological shape and substrate stiffness. *Proc. Natl. Acad. Sci. U. S. A.* **112**, 12705–12710 (2015).
13. Tang, X., Yakut Ali, M. & Saif, M. T. A. A novel technique for micro-patterning proteins and cells on polyacrylamide gels. *Soft Matter* **8**, 7197–7206 (2012).
14. Moeller, J. *et al.* Controlling cell shape on hydrogels using liftoff protein patterning. *PLoS One* **13**, 1–17 (2018).
15. Sarker, B., Walter, C. & Pathak, A. Direct Micropatterning of Extracellular Matrix Proteins on Functionalized Polyacrylamide Hydrogels Shows Geometric Regulation of Cell-Cell Junctions. *ACS Biomater. Sci. Eng.* **4**, 2340–2349 (2018).
16. Nelson, C. M., Raghavan, S., Tan, J. L. & Chen, C. S. Degradation of micropatterned surfaces by cell-dependent and -independent processes. *Langmuir* **19**, 1493–1499 (2003).
17. Kane, R. S., Takayama, S., Ostuni, E., Ingber, D. E. & Whitesides, G. M. Patterning proteins and cells using soft lithography. *Biomaterials* **20**, 2363–2376 (1999).
18. Damljanović, V., Lagerholm, B. C. & Jacobson, K. Bulk and micropatterned conjugation of extracellular matrix proteins to characterized polyacrylamide substrates for cell mechanotransduction assays. *Biotechniques* **39**, 847–851 (2005).
19. Denisin, A. K. & Pruitt, B. L. Tuning the Range of Polyacrylamide Gel Stiffness for Mechanobiology Applications. *ACS Appl. Mater. Interfaces* **8**, 21893–21902 (2016).
20. Loh *et al.* The E-Cadherin and N-Cadherin Switch in Epithelial-to-Mesenchymal

Transition: Signaling, Therapeutic Implications, and Challenges. *Cells* **8**, 1118 (2019).

21. Sheehy, S. P. *et al.* Quality metrics for stem cell-derived cardiac myocytes. *Stem Cell Reports* **2**, 282–294 (2014).
22. Wang, G. *et al.* Modeling the mitochondrial cardiomyopathy of Barth syndrome with iPSC and heart-on-chip technologies. *Nat Med* **20**, 616–623 (2014).
23. Li, Y. *et al.* The N-cadherin interactome in primary cardiomyocytes as defined using quantitative proximity proteomics. *J. Cell Sci.* **132**, (2019).
24. Parker, K. K., Tan, J., Chen, C. S. & Tung, L. Myofibrillar architecture in engineered cardiac myocytes. *Circ. Res.* **103**, 340–342 (2008).
25. Roberts, B. *et al.* Fluorescent Gene Tagging of Transcriptionally Silent Genes in hiPSCs. *Stem Cell Reports* **12**, 1145–1158 (2019).
26. Roberts, B. *et al.* Systematic gene tagging using CRISPR/Cas9 in human stem cells to illuminate cell organization. *Mol. Biol. Cell* **28**, 2854–2874 (2017).
27. Knöll, R., Buyandelger, B. & Lab, M. The sarcomeric Z-disc and Z-discopathies. *J. Biomed. Biotechnol.* **2011**, (2011).
28. Sharma, A. *et al.* Derivation of highly purified cardiomyocytes from human induced pluripotent stem cells using small molecule-modulated differentiation and subsequent glucose starvation. *J. Vis. Exp.* **2015**, 52628 (2015).
29. Notbohm, J. *et al.* Two-Dimensional Culture Systems to Enable Mechanics-Based Assays for Stem Cell-Derived Cardiomyocytes. *Exp. Mech.* (2019) doi:10.1007/s11340-019-00473-8.
30. Ribeiro, M. C. *et al.* A cardiomyocyte show of force: A fluorescent alpha-actinin reporter line sheds light on human cardiomyocyte contractility versus substrate stiffness. *J. Mol.*

Cell. Cardiol. **141**, 54–64 (2020).

31. Chen, W., Shao, Y., Li, X., Zhao, G. & Fu, J. Nanotopographical surfaces for stem cell fate control: Engineering mechanobiology from the bottom. *Nano Today* **9**, 759–784 (2014).

32. Abadi, P. P. S. S. *et al.* Engineering of Mature Human Induced Pluripotent Stem Cell-Derived Cardiomyocytes Using Substrates with Multiscale Topography. *Adv. Funct. Mater.* **28**, 1–11 (2018).

33. Nag, K., Adnan, N., Kutsuzawa, K. & Akaike, T. Cadherin-Fc Chimeric Protein-Based Biomaterials: Advancing Stem Cell Technology and Regenerative Medicine Towards Application. in *Pluripotent Stem Cell Biology - Advances in Mechanisms, Methods and Models* (2014). doi:10.5772/58287.

34. Yue, X. S. *et al.* A fusion protein N-cadherin-Fc as an artificial extracellular matrix surface for maintenance of stem cell features. *Biomaterials* **31**, 5287–5296 (2010).

35. Baumgartner, W. *et al.* Cadherin interaction probed by atomic force microscopy. *Proc. Natl. Acad. Sci. U. S. A.* **97**, 4005–4010 (2000).

36. Pasche, S., De Paul, S. M., Vörös, J., Spencer, N. D. & Textor, M. Poly(l-lysine)-graft-poly(ethylene glycol) Assembled Monolayers on Niobium Oxide Surfaces: A Quantitative Study of the Influence of Polymer Interfacial Architecture on Resistance to Protein Adsorption by ToF-SIMS and in Situ OWLS. *Langmuir* **19**, 9216–9225 (2003).

37. Di Benedetto, F., Biasco, A., Pisignano, D. & Cingolani, R. Patterning polyacrylamide hydrogels by soft lithography. *Nanotechnology* **16**, (2005).

38. Ribeiro, A. J. S., Denisin, A. K., Wilson, R. E. & Pruitt, B. L. For whom the cells pull: Hydrogel and micropost devices for measuring traction forces. *Methods* **94**, 51–64 (2016).

39. Li, X., Meng, G., Krawetz, R., Liu, S. & Rancourt, D. E. The ROCK inhibitor Y-27632 enhances the survival rate of human embryonic stem cells following cryopreservation. *Stem Cells Dev.* **17**, 1079–1085 (2008).

40. Denisin, A. K. Controlling the Microenvironment to Investigate Single Cell Mechanobiology, Adhesion, and Function. (Stanford University, 2018).

41. Collins, C., Denisin, A. K., Pruitt, B. L. & Nelson, W. J. Changes in E-cadherin rigidity sensing regulate cell adhesion. *Proc. Natl. Acad. Sci. U. S. A.* **114**, E5835–E5844 (2017).